scientific reports

Check for updates

OPEN

Chronic environmental temperature affects protein expression in the eye of adult zebrafish (*Danio rerio*)

Elisa Maffioli[1,5], Simona Nonnis[1,2,5], Francesca Grassi Scalvini[1], Joshua Grana[1], Armando Negri[1], Flavia Frabetti[3], Gabriella Tedeschi[1,2]✉ & Mattia Toni[4]✉

Vision in vertebrates is mediated by the eye, a complex organ with developmental and functional similarities to the central nervous system. Eye proteomics has emerged as a powerful tool for investigating ocular function and disease mechanisms, including neurodegeneration and ocular toxicity. The zebrafish (*Danio rerio*) is a well-established model in biomedical research, including ophthalmology, due to its highly developed visual system, rapid eye maturation, and genetic homology with humans. Building on previous findings that thermal stress can affect neural tissues, this study investigates whether prolonged exposure to non-optimal temperatures also impacts the zebrafish eye proteome. Adult zebrafish were maintained for 21 days at elevated (34 °C), control (26 °C), or low (18 °C) temperatures, and eye proteomes were analysed by tandem mass spectrometry. Our results reveal that both low and high temperatures induce distinct alterations in the expression of proteins involved in critical eye processes. Notably, high-temperature exposure modulates pathways such as sirtuin signalling while downregulating proteins involved in oxidative phosphorylation, electron transport, and ATP synthesis, alongside decreased expression of proteins central to visual phototransduction. These data indicate that environmental temperature can directly impact eye protein homeostasis, supporting a potential role for the thermal stress in ocular dysfunction.

Vision in vertebrates is mediated by the eyes, complex sensory organs that originate from three distinct embryonic tissues: the neuroectoderm, surface ectoderm, and mesenchyme[1]. The retina, the neural component of the eye, develops from the embryonic neural tube, similarly to the brain and spinal cord. During embryogenesis, the diencephalic region of the neural tube, which expresses key eye-field transcription factors, expands bilaterally to form the optic vesicles, which give rise to the neuronal structures of the eye[2,3].

The vertebrate retina comprises seven major cell types, organised into three nuclear layers separated by two synaptic (plexiform) layers[2]. Among these are rods and cones, the photoreceptors responsible for capturing light and initiating signal transduction. Retinal ganglion cells project axons to brain targets via the optic nerve. Bipolar, horizontal, and amacrine cells refine and relay visual information to ganglion cells. Müller glial cells support retinal architecture and homeostasis. In addition, astrocytes, microglia, and cells of the retinal vasculature contribute to the overall retinal microenvironment[2]. Vascular endothelial cells and pericytes, for example, form the inner blood–retinal barrier, regulate capillary blood flow, and contribute to angiogenesis[4,5].

The field of eye proteomics, particularly retinal proteomics, is rapidly evolving, offering crucial insights into the protein dynamics underlying ocular function and disease[6–9]. Proteomic analyses have significantly contributed to elucidating molecular mechanisms involved in the pathogenesis, diagnosis, and treatment of ocular disorders, as exemplified by the launch of the Human Eye Proteome Project in 2013[7]. Furthermore, due to its shared cellular and molecular features with the central nervous system, the retina serves as a valuable model for studying neurodegenerative conditions such as Alzheimer's disease[9].

[1]Department of Veterinary Medicine and Animal Science (DIVAS), Università degli Studi di Milano, Via dell'Università 6, Lodi 26900, Italy. [2]CRC"Innovation for Well-Being and Environment" (I-WE), Università degli Studi di Milano, Milano 20126, Italy. [3]Department of Medical and Surgical Sciences—DIMEC, University of Bologna, Bologna 40126, Italy. [4]Department of Biology and Biotechnologies "Charles Darwin", Sapienza University, Rome 00185, Italy. [5]Elisa Maffioli and Simona Nonnis contributed equally to this work. ✉email: gabriella.tedeschi@unimi.it; mattia.toni@uniroma1.it

Environmental stressors are now recognised as important risk factors for ocular diseases, and air pollution, toxic metals, and climate-related factors have been linked to conditions such as cataracts, age-related macular degeneration, uveitis, and dry eye syndrome[10]. So, retinal proteomics also plays a key role in evaluating ocular toxicity by assessing drug-induced and environmental impacts on retinal health, changes that can ultimately result in vision loss[11].

The zebrafish (*Danio rerio*), a freshwater cyprinid, has emerged as a valuable model organism owing to its ease of maintenance, low cost, fully annotated genome, high genetic homology with humans, and transparent embryos[12] that facilitate detailed molecular analyses, such as tissue-specific proteomic profiling. These features, combined with advanced colour vision and a strong reliance on sight, make zebrafish particularly suitable for ophthalmological studies[1]. Their retinas are anatomically and functionally comparable to those of humans, including a similar abundance of cone photoreceptors. Eye development is also rapid, with the retina reaching functional maturity by around 72 h post-fertilisation (hpf), when robust visual responsiveness becomes evident[1]. Notably, light sensitivity emerges much earlier: non-visual photoreceptive cells can detect light from 5 hpf, the pineal organ is photosensitive by 24 hpf, and retinal photoreception develops between 48 and 72 hpf[13].

Zebrafish are increasingly employed as models for ocular toxicity, with studies conducted in both larvae and adults[14]. A wide range of contaminants including endocrine disruptors, flame retardants, pharmaceuticals, microplastics, agrochemicals, and heavy metals has been shown to impair retinal structure, induce oxidative stress, and alter the expression of phototransduction-related genes[14,15]. Recent studies further highlight the ecological sensitivity of zebrafish ocular tissues to environmental stressors. Polystyrene nanoplastics accumulate in the developing eye and rapidly induce oxidative stress, apoptosis, and dysregulation of genes involved in retinal development and antioxidant defence, ultimately impairing visual performance in larvae[16]. Similarly, environmentally relevant nitrate and nitrite exposure disrupts retinal morphology, alters the expression of key apoptotic and antioxidant markers, and diminishes visually guided behaviours in adults[17]. Together, these findings indicate that the zebrafish retina acts as a highly responsive environmental sensor capable of detecting and integrating diverse chemical challenges. This ocular sensitivity provides strong ecological and translational justification for investigating whether other environmental variables, such as sustained temperature changes, may likewise affect retinal homeostasis.

A growing body of research shows that zebrafish naturally inhabit environments characterised by substantial thermal variability, making them both ecologically and physiologically suitable models for studying the consequences of temperature fluctuations on biological systems. These findings highlight the sensitivity of the visual system to environmental challenges and support the rationale for exploring temperature-induced effects on retinal proteostasis.

Our research group has been investigating the effects of temperature on the zebrafish nervous system for several years. Zebrafish were selected as a model for thermal stress studies due to their broad thermal tolerance, with viable temperature ranges spanning from 6 °C to 43 °C, and tolerable limits between 4.5 °C and 42 °C[18–20]. This remarkable thermal adaptability reflects the natural habitat of zebrafish in South Asia, where daily temperature fluctuations of approximately 5 °C and seasonal shift from around 6 °C in winter to over 38 °C in summer are common[21,22]. Zebrafish typically inhabit brooks, lakes, ponds, and rice fields[23,24], where water temperatures generally range from 16.5 °C to 34.0°C[25]. These ecological characteristics make zebrafish an ideal model for investigating the biological effects of prolonged exposure to environmentally relevant elevated and low temperatures[25].

Our previous studies have shown that both acute (4-day) and chronic (21-day) exposure of adult zebrafish to elevated (34 °C) and low (18 °C) temperatures result in significant changes in brain proteome composition and behaviour, compared to fish maintained at 26 °C[26–29]. These temperatures were selected based on the work of Vergauwen et al.[30], as they fall within the species' viable thermal range and represent ecologically realistic cold and warm conditions. The control temperature of 26 °C was chosen to reflect the zebrafish thermal preferendum[18].

The zebrafish brain response to altered temperature involves a complex network of molecular events, including regulation of neurotrophins such as Brain-Derived Neurotrophic Factor (BDNF)[31] and alterations in the brain lipidome[32]. Together, these findings support the neurotoxic effects of prolonged exposure to both warm and cold temperatures in adult zebrafish, highlighting the broader consequences of thermal stress on neural homeostasis and function[33,34].

In this context, the zebrafish eye offers a compelling model for studying temperature-dependent proteomic changes. Unlike many mammalian models, adult zebrafish rely heavily on vision and possess cone-rich retinas that closely resemble those of humans, thereby enabling translationally relevant investigations.

Although the zebrafish is gaining prominence in vision research, direct investigations into how chronic thermal stress affects the adult eye proteome remain limited.

This study aims to fill this knowledge gap by examining whether prolonged exposure to constant but ecologically relevant elevated (34 °C), control (26 °C), and low (18 °C) temperatures modifies the proteomic landscape of the zebrafish eye.

Building on previous findings showing differential effects of warm and cold temperatures on the zebrafish brain at the levels of proteome, lipidome, and behaviour, we hypothesise that similar thermal conditions may also impact retinal neural function. These effects could influence visual capacity, with distinct outcomes under low and high temperature regimes. Such findings may provide a basis for understanding how thermal stress influences eye health in ectotherms, while offering insights into conserved molecular mechanisms of ocular neurotoxicity with potential relevance for human disease.

Results and discussion

Proteomic effects of constant thermal conditions in the zebrafish eye

The eyes of adult zebrafish maintained for 21 days at 34 °C, 26 °C, and 18 °C were analysed using a shotgun proteomic approach to assess the impact of the exposure to elevated and low temperatures on protein expression. A total of 685 proteins were detected at 34 °C, 683 at 26 °C, and 691 at 18 °C (Fig. 1, Supplementary Tables S1–S3). As shown in the Venn diagram (Fig. 1A), only a limited number of proteins were exclusively expressed at each temperature (15 at 34 °C, 9 at 26 °C, and 12 at 18 °C). However, a Principal Component Analysis (PCA) demonstrated clear clustering by temperature, with the most pronounced separation observed at 34 °C (Fig. 1B).

Multivariate analysis of variance (MANOVA), applied as an exploratory analysis to identify general proteomic patterns among groups, indicates differences across temperature groups (Wilks' $\lambda = 0.0748$, $F(1740, 5236) = 4.134$, $p < 1 \times 10^{-300}$; Pillai's trace = 1.51, $F(1740, 5241) = 3.055$, $p = 1.41 \times 10^{-207}$) in keeping with the proteomic results.

Specific analyses were carried out by comparing 34 °C vs. 26° C and 18 °C vs. 26 °C, with 26 °C kept as the control temperature, as well as by comparing 34 °C vs. 18 °C (Fig. 1C). The lists of proteins differently expressed are provided in the supplementary material (Supplementary Tables S4–S6) reporting the common proteins in the pairwise comparisons whose differential expression is statistically significant according to Student's test and

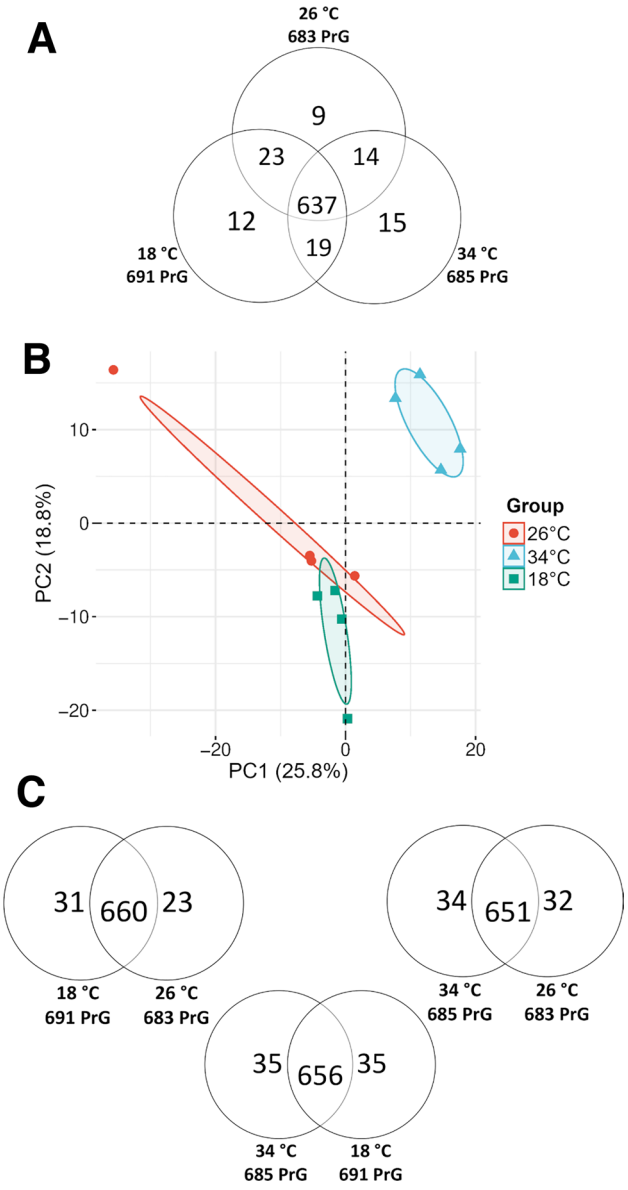

Fig. 1. Proteomic analysis of the zebrafish eye at three different temperatures. A shotgun proteomics approach was applied to the eye of adult zebrafish acclimated for 21 days to three thermal conditions: elevated temperature (34 °C), control temperature (26 °C), and low temperature (18 °C). (**A**) Venn diagram comparing the proteomic datasets across the three temperature conditions. PrG: proteins identified by LC–MS/MS analysis. (**B**) PCA of the three proteomes with confidence ellipses. (**C**) Venn diagram of all the proteins identified in pairwise comparisons: 34 °C vs. 26 °C, 18 °C vs. 26 °C, and 34 °C vs. 18 °C.

also the proteins exclusively expressed at each of the temperatures tested. The proteins listed in Tables S4-S6 were further analysed using an Ingenuity Pathway Analysis (IPA) (Figs. 2 and 3) and Cytoscape (Fig. 4) to identify potential patterns and networks affected by elevated and low temperature.

High temperature (34 °C vs. 26 °C)

At 34 °C, a complex pattern of molecular alterations emerged, affecting multiple pathways in a highly specific manner (Figs. 2A and 3A,B; Table 1).

Heat-induced stress signalling and translational reprogramming

Protein kinase R (PKR), a ubiquitous intracellular stress sensor implicated in the heat-shock response and broader cellular stress signalling[35–37], was activated together with the Eukaryotic Initiation Factor 2 (IF2) and sirtuin signalling, reflecting an adaptive attempt to maintain homeostasis (Figs. 2A and 3B).

Sirtuins, a conserved family of histone deacetylases, are pivotal regulators of cellular stress responses through protein acetylation[38,39]. Seven isoforms are strongly expressed in the zebrafish retina[40], where they protect against oxidative and genotoxic stress via transcriptional regulation and protein deacetylation[41–45]. In particular, SIRT1 protects against NMDA-induced retinal damage when activated by resveratrol[40]. Notably, SIRT1 interacts with and deacetylates eIF2α, thereby constraining its phosphorylation[46–48]. Since eIF2α phosphorylation is central to the integrated stress response[49], attenuating protein synthesis and promoting adaptation[50], our finding of increased PKR signalling[50] is consistent with activation of this axis. Importantly, PKR–eIF2α signalling has been linked to stress granule formation and neurodegeneration[51,52]. The concurrent up-regulation of translation initiation and elongation pathways suggests Integrated Stress Response-driven translational reprogramming[53–55] (Fig. 2A).

Synaptic signalling and neuronal connectivity

The concomitant up-regulation of SNARE signalling and synaptogenesis may reflect an adaptive attempt to sustain neurotransmission and maintain photoreceptor–retinal circuitry under heat stress (Fig. 2A). Indeed, in rodents SNAP-25, a core SNARE complex protein, modulates retinal wave activity and retinogeniculate circuit refinement during development[56]. However, the retina's exceptionally high metabolic demand suggests that persistent activation of these pathways is energetically burdensome and may lead to aberrant synaptic remodelling, ultimately compromising synaptic efficiency and retinal integrity[57].

Mitochondrial impairment and metabolic shift

Mitochondrial-related processes—including oxidative phosphorylation, electron transport, ATP synthesis and heat production by uncoupling proteins, the TCA cycle, and mitochondria protein import—were consistently down-regulated, pointing to impaired mitochondrial activity (Fig. 2A; Table 1). Sirtuins modulation may also be involved as they are known regulators of mitochondrial homeostasis[58], with SIRT3 in particular supporting oxidative phosphorylation and redox balance[59–61]. Causal network analysis of the proteins differentially expressed in the 34 °C vs. 26 °C (Supplementary Table S5) identified highly connected networks associated with retinal and neurological disease, lipid metabolism, and molecular transport. Merged networks are shown in Fig. 3A, while Fig. 3B summarises the principal processes altered at 34 °C. Cytoscape confirmed up-regulation of glycolysis, lipid biosynthesis, and hypoxia response and protein folding (Fig. 4A), alongside down-regulation of oxidative phosphorylation, and energy production (Fig. 4B). Thus, impaired mitochondrial function likely reduces energy availability, while increased glycolysis may act as a compensatory mechanism. Similar heat-induced metabolic shifts towards glycolysis have been reported in other systems[62–64]. Reduced expression of precursor-generating pathways further supports the idea of heat-driven metabolic reprogramming in ocular cells. In parallel, lipid biosynthetic processes were up-regulated, indicating altered lipid composition in ocular tissue. This aligns with lipidomic analyses of the zebrafish brain at 34 °C, which revealed major shifts in lipid content[32], suggesting lipid metabolism is more strongly affected by heat than by cold exposure.

In the context of ocular physiology, suppression of oxidative phosphorylation is expected to have direct consequences for ATP-dependent visual processes. The vertebrate retina is one of the most metabolically demanding tissues in the body, with photoreceptors relying predominantly on mitochondrial ATP to sustain phototransduction, maintain ion gradients through Na^+/K^+-ATPases, and support the continuous renewal of outer-segment discs[65,66]. Mitochondria located in the ellipsoid region of photoreceptors are particularly critical for maintaining the high ATP flux required for dark current maintenance and cyclic nucleotide turnover[67–69].

Similarly, synaptic transmission within the retina, especially at ribbon synapses, requires substantial ATP to fuel vesicle cycling, neurotransmitter release, and Ca^{2+} homeostasis[70]. A heat-induced reduction in mitochondrial energy production is therefore likely to compromise these essential processes, forcing retinal cells to rely more heavily on glycolysis. Although increased glycolytic activity may provide partial metabolic compensation, glycolysis alone is generally insufficient to meet the extremely high energetic demands of photoreceptors and retinal interneurons[71].

This energetic imbalance may contribute to the modulation of retinal protein markers observed at 34 °C. Together, these considerations support the hypothesis that heat-induced mitochondrial dysfunction disrupts ATP availability, potentially affecting phototransduction efficiency, synaptic signalling, and overall retinal performance under elevated temperature.

Compromised phototransduction and visual processing

Proteins associated with visual perception and phototransduction were markedly down-regulated (Figs. 2A, 3B and 4B; Table 1; Supplementary Fig. S1), suggesting that prolonged heat exposure compromises retinal visual processing. This effect is likely attributable to mitochondrial impairment and the consequent reduction in

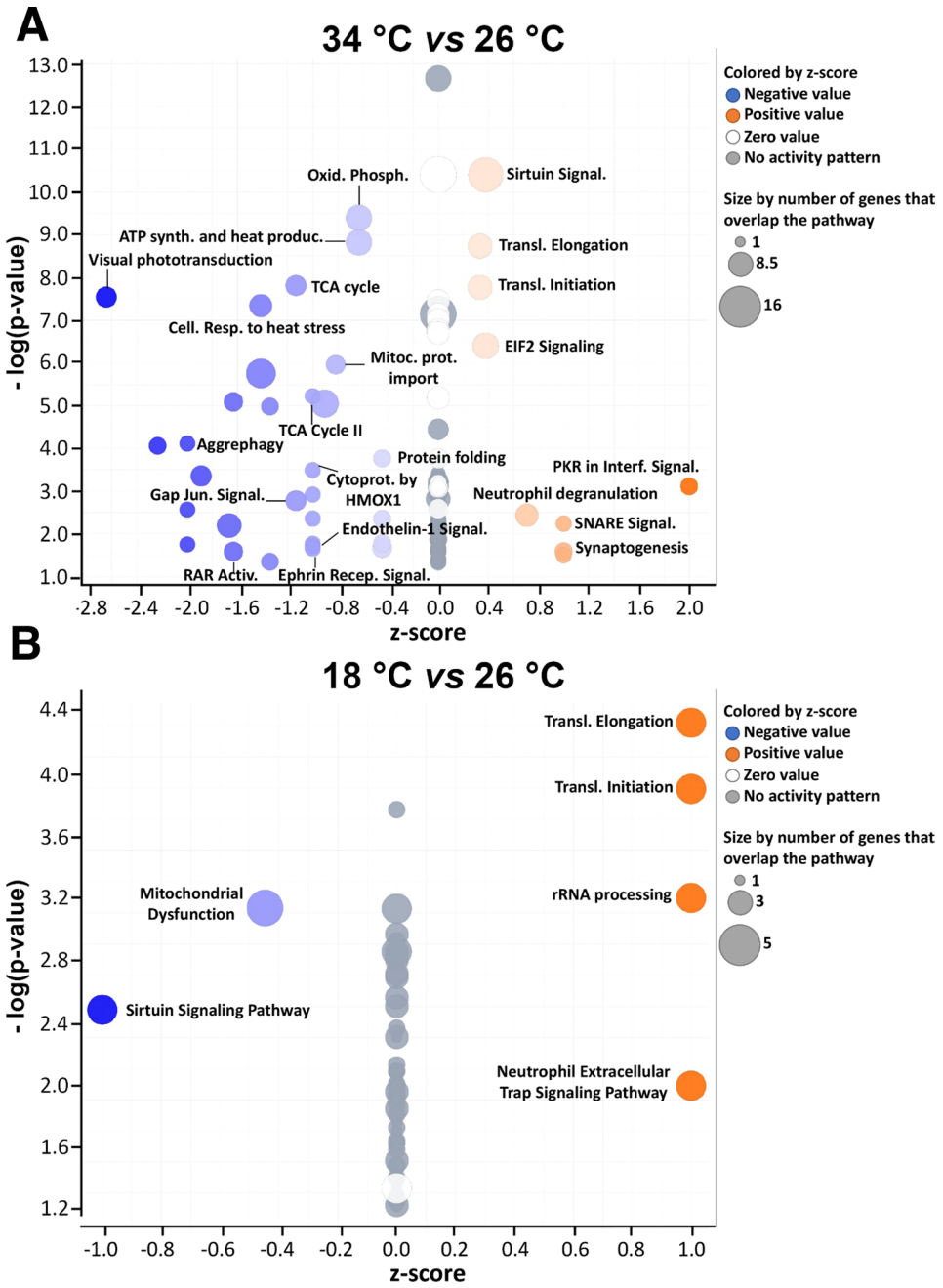

Fig. 2. Canonical pathway analysis of differentially expressed proteins at elevated (34 °C) and low (18 °C) temperatures compared to the control (26 °C) using IPA. Proteins differentially expressed in the 34 °C vs. 26 °C (**A**) and 18 °C vs. 26 °C (**B**) comparisons were analysed using IPA to identify all the most significantly altered canonical pathways. Proteins were considered differentially expressed if they were either uniquely present in one condition or exhibited a statistically significant difference in expression (Student's test FDR ≤ 0.05). For clarity, only a subset of pathways are labelled in each volcano plot. The Z-score indicates the predicted activation or inhibition state of a canonical pathway: with positive scores (orange) indicating activation and negative scores (blue) indicating inhibition. The legend provides details on symbol colours and sizes. Volcano plot of the canonical pathways in the 34 °C vs. 26 °C (**A**) and in 18 °C vs. 26 °C (**B**) comparison, with Z-scores plotted against -log(p-values).

energy availability induced by thermal stress. Strikingly, proteomic analyses in patients with Alzheimer's disease have likewise revealed suppression of photoreceptor activity, oxidative phosphorylation, and mitochondrial function[9]. Such parallels strengthen the hypothesis that heat stress perturbs ocular physiology in a manner reminiscent of neurodegenerative pathology.

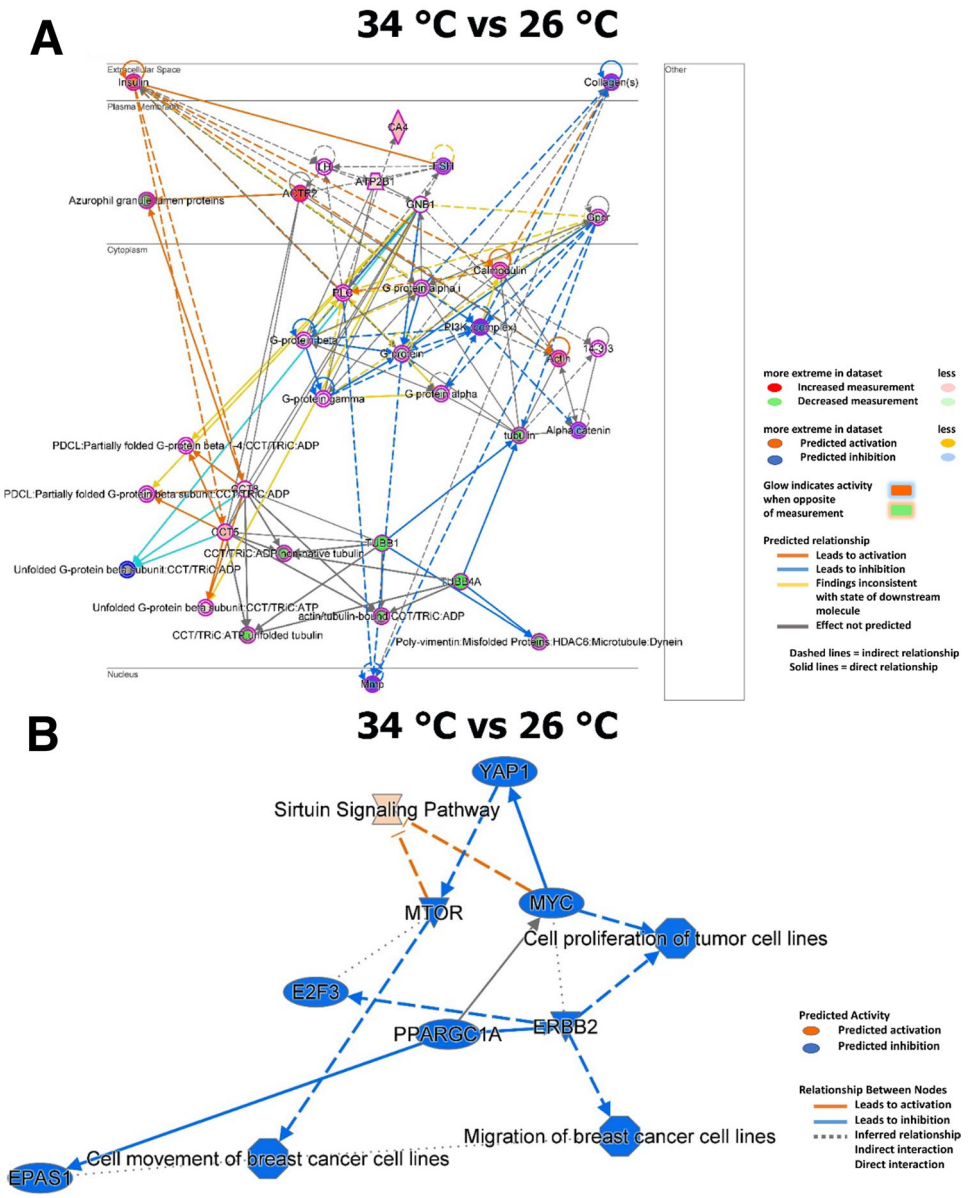

Fig. 3. Bioinformatic analysis of differentially expressed proteins at high temperature (34 °C) compared to the control (26 °C) using IPA. (**A**) Merged network analysis combining the neurological network and the lipid metabolism network. Proteins identified in our dataset are coloured in green. The legend provides details on all other symbols. (**B**) Graphical summary providing a high-level overview of the major biological themes and most significant entities predicted by IPA for differentially expressed proteins in the 34 °C vs. 26 °C comparison.

Defective proteostasis and neurodegeneration-like alterations

Proteomic analysis revealed an up-regulation of chaperone-mediated protein folding (Fig. 3A), together with a concomitant reduction in global protein folding capacity and in aggrephagy (Fig. 2A), a selective autophagy pathway responsible for the clearance of misfolded proteins. Impaired aggrephagy has been associated with reduced proteostatic capacity and the accumulation of protein aggregates in neurodegenerative contexts[72,73]. Indeed, defective aggrephagy is a recognised hallmark of proteinopathies such as Alzheimer's and Huntington's disease[74,75].

A possible cellular scenario suggested by these results is that, although cells attempt to counteract proteotoxic stress by enhancing chaperone activity, their overall proteostatic machinery remains insufficient. In this context, misfolded proteins may be more prone to persist, while their clearance via selective autophagy is reduced. Such an imbalance in protein homeostasis could represent a critical mechanism by which heat stress affects ocular neurons.

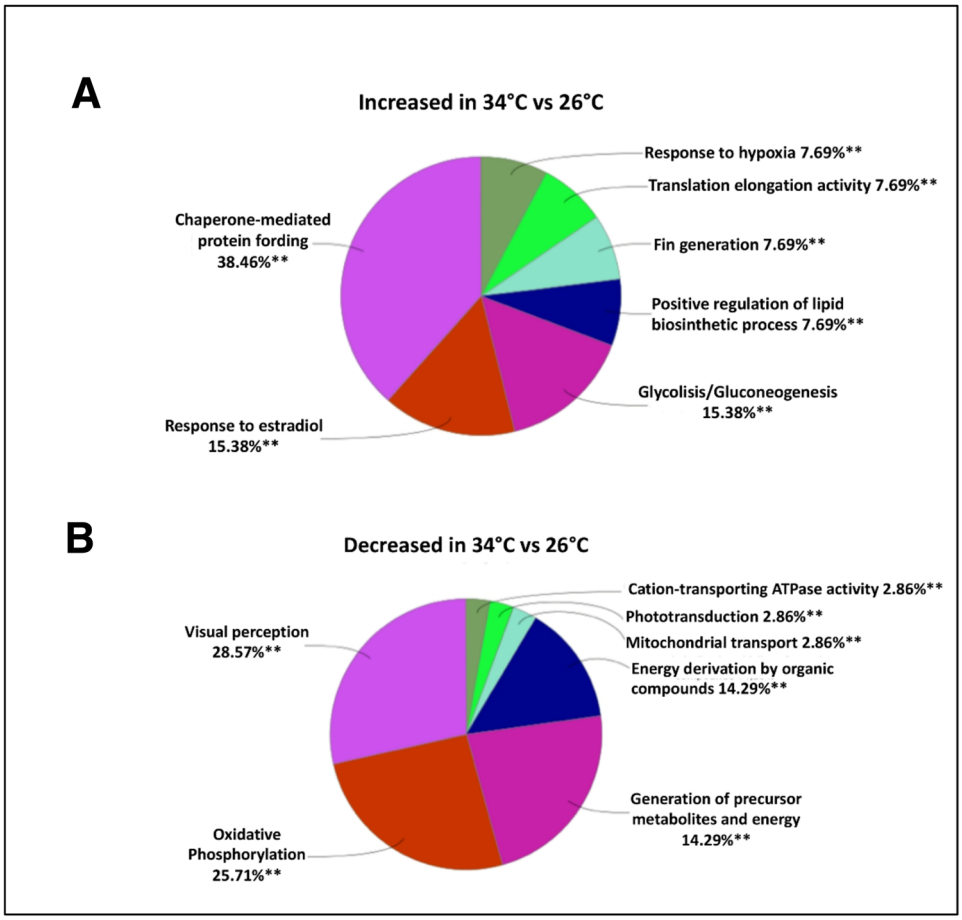

Fig. 4. Bioinformatic analysis of differentially expressed proteins at elevated temperature (34 °C) compared to the control (26 °C) using Cytoscape. A bioinformatic analysis was conducted using CLUEGO software (Cytoscape release 3.8.2) to cluster enriched annotation groups of biological processes, pathways, and networks within the set of differentially expressed proteins in the 34 °C vs. 26 °C comparison. Proteins were considered differentially expressed if they were either uniquely present in one condition or exhibited a statistically significant difference in expression (Student's test FDR ≤ 0.05). Functional grouping of these proteins was then performed using Fisher's exact test (p-value ≤ 0.05, with a minimum of three counts per category). (**A**) Proteins that were upregulated or uniquely expressed at 34 °C. (**B**) Proteins that were downregulated at 34 °C or uniquely expressed at 26 °C.

From molecular changes to behavioural outcomes

Although the observed molecular alterations at 34 °C suggest impaired eye function, they do not directly demonstrate reduced vision. Behavioural changes previously reported in zebrafish exposed to 34 °C for 21 days, including increased boldness and reduced anxiety-like responses[27,28], may reflect brain-driven processes but could also be influenced by impaired retinal input. Reduced phototransduction efficiency might compromise environmental perception and contribute to these behavioural outcomes. Our findings highlight variations in the ocular proteome, including proteins of lens, cornea, and retina, therefore further studies explicitly assessing retinal function and visual performance are warranted.

Low temperature (18 °C vs. 26 °C)

The five most affected pathways at 18 °C were translation elongation, translation initiation, lysine catabolism, rRNA processing, and mitochondrial dysfunction (Table 1).

Translational control and RNA processing

At 18 °C, the IPA revealed strong activation of translation and rRNA processing pathways (Fig. 2A; Table 1), consistent with the role of translational control in thermal adaptation[76,77]. Adjustments of ribosome activity and RNA pools are common in ectothermic organisms adapting to energetic constraints. PCA analysis (Fig. 1B) further confirmed a global reorganisation of protein expression under cold exposure.

Stress signalling and mitochondrial function

Unlike the response observed at 34 °C, sirtuin signalling was inhibited at low temperature (Fig. 2B; Table 1). Given the established roles of sirtuins in genome stability, metabolic adaptation, and mitochondrial stress

EYE PROTEOME				
34 °C vs 26 °C				
Ingenuity canonical pathways	**-log(p-value)**	**p-value**	**z-score**	**Molecules**
Visual phototransduction	5.82	1.51E-06	-2.65	GNAT1,GNB1,GRK1,OPN1LW,OPN1SW,RPE65,SAG
Mitochondrial dysfunction	8.21	6.23E-09	0.00	ATP1A3,ATP5F1C,CAPNS1,COX4I1,COX6C,COX7A2L,CYC1,DLAT,IDH2,NDUFA9,NDUFB10,NDUFV1,UQCRC2,UQCRFS1,VDAC1,VDAC2
Sirtuin signaling pathway	8.21	6.23E-09	0.38	ATP5F1C,CYC1,GLS,IDH2,LDHA,NDRG1,NDUFA9,NDUFB10,NDUFV1,PGK1,SLC25A5,UQCRC2,UQCRFS1,VDAC1,VDAC2
Oxidative phosphorylation	7.32	4.78E-08	-0.63	ATP5F1C,COX4I1,COX6C,COX7A2L,CYC1,NDUFA9,NDUFB10,NDUFV1,UQCRC2,UQCRFS1
Electron transport, ATP synthesis, and heat production by uncoupling proteins	8.82	1.51E-09	-0.63	ATP5F1C,COX4I1,COX6C,COX7A2L,CYC1,NDUFA9,NDUFB10,NDUFV1,UQCRC2,UQCRFS1
18 °C vs 26 °C				
Ingenuity canonical pathways	**-log(p-value)**	**p-value**	**z-score**	**Molecules**
Eukaryotic translation elongation	2.00	1.04E-02	1.00	EEF1G,RPL19,RPL6,RPS19
Eukaryotic translation initiation	1.90	1.25E-02	1.00	EIF4A1,RPL19,RPL6,RPS19
Lysine catabolism	1.902	1.25E+02	0.00	ALDH7A1,OGDH
Major pathway of rRNA processing in the nucleolus and cytosol	1.57	2.70E-02	1.00	NCL,RPL19,RPL6,RPS19
Mitochondrial dysfunction	1.57	2.70E-02	-0.45	HSD17B10,NDUFA9,NDUFS3,OGDH,SOD2
34 °C vs 18 °C				
Ingenuity canonical pathways	**-log(p-value)**	**p-value**	**z-score**	**Molecules**
Phototransduction pathway	10.39	4.13E-11	0.632	ARR3,GNAT1,GNAT2,GNB1,GNGT1,GRK1,OPN1LW,OPN1SW,PDC,SAG
Mitochondrial dysfunction	10.38	4.13E-11	2.36	ATP1A3,CAPNS1,COX4I1,COX6C,COX7A2L,CYC1,DLAT,GSTP1,HSD17B10,MT-CO2,NDUFB10,NDUFS1,NDUFS3,NDUFV1,OGDH,SOD1, SOD2,UQCR10
Oxidative phosphorylation	7.33	4.69E-08	-3.16	COX4I1,COX6C,COX7A2L,CYC1,MT-CO2,NDUFB10,NDUFS1,NDUFS3,NDUFV1,UQCR10
Visual phototransduction	7.06	8.07E-08	-2.83	GNAT1,GNB1,GNGT1,GRK1,OPN1LW,OPN1SW,RPE65,SAG
Electron transport, ATP synthesis, and heat production by uncoupling proteins	9.56	1.14E-09	-3.16	COX4I1,COX6C,COX7A2L,CYC1,MT-CO2,NDUFB10,NDUFS1,NDUFS3,NDUFV1,UQCR10

Table 1. Top five most significantly altered pathways in the zebrafish eye at three different temperatures. An Ingenuity Pathway Analysis (IPA) was performed on the eye of adult zebrafish acclimated for 21 days to three thermal conditions: elevated temperature (34 °C), control temperature (26 °C), and low temperature (18 °C). The table lists the five most significantly altered canonical pathways identified by IPA in each pairwise comparison. Proteins were considered differentially expressed if they were either uniquely present in one condition or exhibited a statistically significant difference in expression (Student's test FDR≤ ≤ 0.05). The significance value represents the probability that the association between a given dataset and a canonical pathway occurred by random chance. P-value = B-H adjusted p value.

responses[78,79], as well as their documented contribution to thermal tolerance in marine ectotherms such as the blue mussels *Mytilus galloprovincialis* and *Mytilus trossulus*[80], this down-regulation suggests that cold exposure demands fewer stress-protective mechanisms than heat stress.

At 18 °C temperature, the mitochondrial dysfunction pathway was inhibited exhibiting a negative Z-score (− 0.45), and no significant alterations in oxidative phosphorylation, electron transport, or ATP synthesis. This indicates that mitochondrial integrity is better preserved at low temperatures than under high-temperature stress. Such a response is consistent with the reduced metabolic rate characteristic of cold conditions and supports the view that mitochondrial plasticity underpins cold tolerance in fish[81,82].

Global proteomic organisation

Unlike the 34 °C vs. 26 °C comparison, the IPA did not generate a graphical summary for the 18 °C vs. 26 °C dataset (Fig. 3B), likely due to too few high-confidence entities. This supports the view that heat drives the most extensive proteomic reorganisation, while cold elicits a subtler but distinct response. Cytoscape analysis corroborated this as no significant pathway associations were found at 18 °C (Fig. 4A,B), whereas 34 °C induced strong up-regulation of protein folding, glycolysis, lipid biosynthesis, and hypoxia response (Fig. 4A), along with down-regulation of visual perception, phototransduction, oxidative phosphorylation, and energy production (Fig. 4B).

Direct comparison of extreme conditions (34 °C vs. 18 °C)

The 34 °C vs. 26 °C and 18 °C vs. 26 °C comparisons revealed distinct effects of elevated and low temperatures on the zebrafish eye. Collectively, these findings show that chronic heat stress induces major metabolic and functional remodelling, whereas cold stress primarily results in subtler adjustments of protein synthesis and mitochondrial activity. The separation along PCA component 1 (Fig. 1B) further confirms that 34 °C has a stronger effect on ocular function and vision than 18 °C.

To further clarify the differences between heat- and cold-induced responses, a direct comparison of the two extreme conditions was performed (34 °C vs. 18 °C). The IPA identified proteins exclusively expressed at one temperature or significantly altered between the two (Supplementary Table S6).

At 34 °C, mitochondrial-related processes were markedly impaired, accompanied by strong inhibition of phototransduction and visual phototransduction pathways, as well as ATP synthesis, heat production by uncoupling proteins, and oxidative phosphorylation (Table 1; Supplementary Fig. S2A). These results suggest that heat exposure compromises mitochondrial efficiency and visual capacity more severely than cold exposure.

Conversely, several pathways were significantly upregulated at 34 °C relative to 18 °C, including sirtuin signalling, mitochondrial dysfunction, heat stress response, collagen biosynthesis, extracellular matrix organisation, and BAG2 signalling (Table 1; Supplementary Fig. S2A,B). This pattern mirrors that observed in the 34 °C vs. 26 °C comparison, reinforcing the notion that heat stress elicits robust adaptive responses, extensive mitochondrial impairment, and profound extracellular remodelling.

Overall, the 34 °C vs. 18 °C comparison underscores the sharper impact of heat relative to cold exposure on the zebrafish eye proteome. While cold conditions induce moderate reorganisation of protein synthesis and stress-related pathways, heat stress severely disrupts mitochondrial processes and visual phototransduction, posing a greater challenge to ocular function and cellular homeostasis. Importantly, comparing the two extremes enables a clear separation of heat- versus cold-specific effects, rather than merely assessing deviations from the control temperature (26 °C). Although such abrupt shifts are uncommon in natural habitats, they provide a critical framework for assessing the boundaries of thermal tolerance and for disentangling the relative contributions of cold and heat stress to ocular physiology.

Shared and distinct proteomic responses to thermal conditions in the zebrafish brain and eye

Although the present study focused on the zebrafish eye, we compared our proteomic findings with previously published brain data obtained under identical thermal conditions (34 °C, 26 °C, and 18 °C for 21 days)[28]. This qualitative analysis was not intended to imply a direct functional equivalence between the two tissues, but rather to explore whether shared molecular signatures of thermal sensitivity might emerge across neural structures of common embryonic origin. The retina derives from the neural tube and is composed of neurons and glial cells, thus representing a peripheral extension of the central nervous system[2,83]. On this basis, we hypothesised that both structures could display overlapping responses to thermal stress while retaining tissue-specific traits.

To address this, we re-analysed the published brain dataset[28] applying the same IPA pipeline and summarising the five most significantly altered canonical pathways under each pairwise thermal comparison (Table 2). We then compared these results with those obtained for the eye (Table 1), focusing on recurring or divergent pathway-level responses between the two tissues. This qualitative comparison highlighted a set of common molecular alterations despite tissue-specific signatures.

Elevated temperature responses

Exposure to elevated temperature elicited broadly convergent molecular disturbances in both brain and eye (Tables 1 and 2; Fig. 5). Upregulation of the sirtuin signalling pathway, often associated with stress coping mechanisms and neuroprotection[84], occurred in parallel with downregulation of mitochondrial oxidative phosphorylation, electron transport, and ATP synthesis—hallmarks of mitochondrial dysfunction under thermal stress[85]. These findings indicate a general decline in energy metabolism and cellular efficiency in response to sustained heat exposure.

In the eye, such alterations were accompanied by a reduction in proteins involved in visual phototransduction, pointing to a possible impairment of retinal physiology and visual capacity. In the brain, previously reported findings[28] highlighted downregulation of synaptic signalling, neurotransmitter secretion, and key regulatory

Brain proteome				
34 °C vs 26 °C				
Ingenuity canonical pathways	**-log(p-value)**	**p-value**	**z-score**	**Molecules**
RHO GTPase cycle	6.21	6,19E-7	-2.98	ACTG1,ARHGEF4,BCAP31,CLTC,CUL3,CYFIP2,DDX39B,ECT2,ELMO2,FGD4,FLOT1,FLOT2,GIT1,GOLGA3,SENP1,SPTAN1,SRGAP1,SRGAP3,STIP1,TPM3,TRIO,TWF1
Sirtuin signaling pathway	5.91	1,22E-06	1.51	H1-6,LDHA,MT-ATP6,NDUFA1,NDUFB7,NDUFB9,NDUFS2,NDUFS4,PRKAA1,SIRT5,SLC25A5,SLC2A1,TIMM13,TIMM8A,TOMM34,TUBA1A,UQCRFS1,VDAC1
Mitochondrial dysfunction	5.86	1,39E-06	0.69	ATP5PO,CACNA2D2,CAPNS1,COX6B1,GSTP1,HSD17B10,MAPK10,MT-ATP6,MT-CO2,NDUFA1,NDUFB7,NDUFB9,NDUFS2,NDUFS4,PRKAA1,TOMM34,UQCRFS1,UQCRQ,VDAC1
Electron transport, ATP synthesis, and heat production by uncoupling proteins	7.62	2,41E-08	-1.73	ATP5PO,COX6B1,ETFDH,MT-ATP6,MT-CO2,NDUFA1,NDUFB7,NDUFB9,NDUFS2,NDUFS4,UQCRFS1,UQCRQ
Oxidative phosphorylation	5.34	4,52E-06	-1.51	ATP5PO,COX6B1,MT-ATP6,MT-CO2,NDUFA1,NDUFB7,NDUFB9,NDUFS2,NDUFS4,UQCRFS1,UQCRQ
18 °C vs 26 °C				
Ingenuity canonical pathways	**-log(p-value)**	**p-value**	**z-score**	**Molecules**
Sirtuin signaling pathway	7.93	1,18E-8	2.00	G6PD,H1-6,LDHA,MT-ATP6,NDUFA1,NDUFB3,NDUFB7,NDUFB9,NDUFS4,OTC,PFKM,PRKAA1,SDHB,SIRT5,SLC2A1,TIMM13,TIMM8A,TOMM34,TUBA1A,TUBA4A,TUBA8,VDAC1
Protein folding	5.92	1,21E-06	-1.16	CSNK2A2,CSNK2A3,GNB1,GNG13,GNG3,PFDN1,PFDN6,TUBA1A,TUBA4A,TUBA8,TUBB1,USP11
Activation of NMDA receptors and postsynaptic events	5.75	1,79E-06	-0.63	ADCY1,CAMK4,DLG2,GIT1,PDPK1,PRKAA1,RASGRF1,TUBA1A,TUBA4A,TUBA8,TUBB1
RHO GTPase cycle	5.073	8,46E-06	-2.98	ACTG1,ARHGEF4,BCAP31,BCR,CLTC,CUL3,CYFIP2,DDX39B,ECT2,ELMO2,FGD4,FLOT1,FLOT2,GIT1,GOLGA3,SENP1,SRGAP1,SRGAP3,STIP1,TPM3,TRIO,TWF1
Mitochondrial dysfunction	5.07	8,05E-06	1.15	ATP1B2,ATP5PO,CAPNS1,COX6B1,GSTP1,HSD17B10,MAPK10,MT-ATP6,MT-CO2,NDUFA1,NDUFB3,NDUFB7,NDUFB9,NDUFS4,PRKAA1,SDHB,TOMM34,UQCRQ,VDAC1

Table 2. Top five most significantly altered pathways in the zebrafish brain at three different temperatures. the IPA was performed on the brain of adult zebrafish acclimated for 21 days to three thermal conditions: elevated temperature (34 °C), control temperature (26 °C), low high temperature (18 °C), based on previously published data[27] data[28]. The table lists the five most significantly altered canonical pathways identified by a new IPA performed on the dataset from[27] from[28]. Proteins were considered differentially expressed if they were either uniquely present in one condition or exhibited a statistically significant difference in expression (Student's test FDR≤ ≤ 0.05). The significance value represents the probability that the association between a given dataset and a canonical pathway occurred by random chance. P-value = B-H adjusted p value.

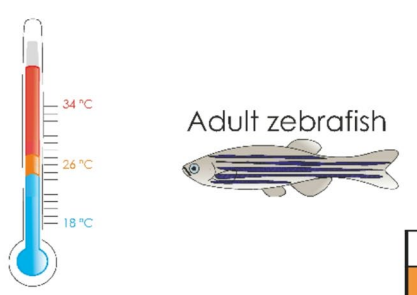

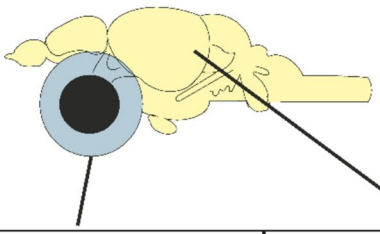

	Eye		Brain	
	34 °C vs 26 °C	18 °C vs 26 °C	34 °C vs 26 °C	18 °C vs 26 °C
Major pathway of rRNA processing		↑↑		
Translation initiation and elongation	↑	↑↑		
Protein folding	0			↓↓
Sirtuin Signaling Pathway	↑	↓↓	↑↑	↑↑
Mitochondrial Dysfunction	0	↓	↑	↑↑
Oxidative Phosphorylation	↓		↓↓	
Electron transport & ATP synthesis	↓		↓↓	
RHO GTPase cycle			↓↓	↓↓
Activation of NMDA receptors				↓
Visual phototransduction	↓↓			

Fig. 5. Key alterations in protein expression in the brain and eye of adult zebrafish exposed to elevated (34 °C, orange) or low (18 °C, blue) temperatures compared with the control (26 °C). The figure summarizes and compares the most significantly enriched pathways identified in the zebrafish eye (Table 1; Fig. 2) and brain (Table 2) after 21 days of acclimation, based on IPA. An upward arrow (↑) denotes IPA-predicted pathway activation, while a downward arrow (↓) denotes inhibition. Zero means no predicted activation/inhibition of the stastistically altered pathways. Single arrows indicate absolute Z-scores > 0 and < 1, whereas double arrows (↑↑/↓↓) represent absolute Z-scores ≥ 1.

cascades (e.g., Ras, PDGF, FGF, Integrin, EGF), all central to neuronal plasticity and intercellular communication. Taken together, these parallel responses across two neural tissues reinforce the view that thermal stress impairs core cellular processes such as mitochondrial integrity and proteostasis, while tissue-specific alterations suggest additional vulnerability of eye physiology.

Low temperature responses

By contrast, responses to cold exposure (18 °C) diverged between the two tissues. While sirtuin signalling was upregulated in the brain, it was downregulated in the eye; markers of mitochondrial dysfunction were increased in the brain but decreased in the retina. These opposite trends suggest that low temperature triggers distinct adaptive strategies in different neural tissues rather than a uniform neuroprotective or neurotoxic response.

Thermal stress, neural resilience, and implications

Overall, our findings indicate that both elevated and reduced constant temperatures can exert neurotoxic effects, albeit through distinct, tissue-specific mechanisms. In the eye, sustained heat stress triggers mitochondrial, proteostatic, and neuronal stress responses, with potential implications for neurodegenerative-like conditions. Conversely, cold exposure does not appear to impair visual phototransduction and may involve different molecular pathways.

Further work is needed to determine whether the observed proteomic differences reflect altered protein expression, protein degradation, or both, as well as to establish the long-term consequences of these changes for neural health in zebrafish and other ectothermic species. Additional studies are also required to test whether the proteomic alterations detected in the brain and eye revert to the control condition when zebrafish exposed to 34 °C or 18 °C for 21 days are subsequently returned to 26 °C.

This aspect is particularly relevant given the known resilience and regenerative capacity of the zebrafish retina[86–88]. Such investigations would clarify whether the proteomic signatures indicative of neurotoxic effects are reversible, and whether different levels of resilience to thermal stress exist between the brain and the eye.

From an ecological perspective, temperature-driven proteomic remodelling in the eye suggests that naturally occurring exposure to low or elevated temperatures within the viable thermal range of zebrafish may compromise visual performance, ultimately affecting behaviour and survival.

At the same time, parallels with molecular disturbances associated with human retinal and neurodegenerative disorders emphasise the translational value of the zebrafish as a model for investigating conserved mechanisms of ocular neurotoxicity.

Conclusions

This study demonstrates that a 21-day exposure to constant elevated (34 °C) and low (18 °C) temperatures, relative to the control (26 °C), significantly alters the proteomic profile of the adult zebrafish eye. Both treatments modulated proteins essential for retinal function, but in clearly distinct ways, confirming that the ocular response to thermal stress is temperature-dependent. Notably, elevated temperature induced proteomic signatures closely resembling those previously described in the zebrafish brain, including the up-regulation of sirtuin signalling and the down-regulation of oxidative phosphorylation, electron transport, and ATP-synthesis pathways. Within the eye, these mitochondrial impairments were accompanied by a robust reduction in visual phototransduction proteins, suggesting a pronounced neurotoxic impact of elevated temperature on eye function. In direct relation to the study's guiding hypothesis, these findings provide strong evidence that chronic thermal exposure differentially disrupts ocular homeostasis, with heat imposing a substantially greater metabolic and functional burden than cold. The marked mitochondrial dysfunction, phototransduction deficits, and activation of stress-related pathways observed at 34 °C—contrasting with the subtler translational and RNA-processing adjustments detected at 18 °C—indicate that elevated temperature is the dominant driver of thermal stress–induced neurotoxic alterations in the zebrafish eye. Taken together, our findings reveal that the adult zebrafish eye is highly sensitive to sustained deviation from the preferred thermal range. By uncovering molecular pathways that are differentially affected underm warm and cold conditions, this work broadens current understanding of temperature-induced neurotoxicity in ectothermic vertebrates and highlights the particular vulnerability of the visual system in the context of global warming.

Methods

Subjects and housing conditions

A total of 96 adult wild-type zebrafish (*Danio rerio*), with an equal male-to-female ratio (1:1) and a mean weight of 0.4 g, were housed in the zebrafish facility at the University of Bologna. The fish were randomly allocated to three identical glass tanks (40 × 30 × 30 cm; width × depth × height), with 32 individuals per tank at a density of 1 fish per litre.

All fish were maintained at a constant temperature of 26 ± 1 °C (control condition) for 10 days to allow acclimatisation. Throughout the experiment, the tanks were kept under a regulated 14:10 h light/dark photoperiod, and the fish were fed three times daily (10 AM, 2 PM, and 6 PM) using automatic feeders (Eden 90, Eden Water Paradise, Germany). A commercial dry granular diet (TropiGranMIX, Dajanapet, Czech Republic) was provided, ensuring a balanced intake according to fish appetite.

Water quality and tank maintenance

Each tank was equipped with an external filtration system (Eden 511 h, Eden s.r.l., Vicenza, Italy), maintaining a constant flow of filtered water (600 L/h). Water was continuously aerated with aquarium aerators (Sicce AIRlight, SICCE s.r.l., Vicenza, Italy; 3300 cc/min, 200 L/h). Temperature was controlled with digital thermostats (Eden 430, Eden s.r.l., Vicenza, Italy), connected to heating coils (Eden 415, 230 V, 50/60 Hz, 80 W, Eden s.r.l., Vicenza, Italy), and supplemented by a cooling system. Daily measurements were performed using calibrated hand thermometers.

The chemical and physical characteristics of the tank water were monitored at least twice per week using a Sera Aqua-Test Box Kit (Sera GmbH, Heinsberg, Germany) and an eSHa Aqua Quick Test (eSHa Lab, Maastricht, The Netherlands). No differences were observed between the treatment and control tanks. Total ammonia (NH_3/NH_4^+) and nitrite (NO_2^-) were consistently below detection limits (0.05 mg/L). Partial water changes were performed whenever nitrate concentrations approached 25 mg/L. The water had a stable pH of 7, conductivity values ranging between 400 and 500 µS/cm, total hardness between 7 and 14 °dH, and carbonate hardness (dKH) of 6. Phosphate (PO_4^{3-}) concentrations remained below 1 mg/L, and neither copper (Cu) nor chlorine (Cl_2) was detected. Overall, water quality parameters remained constant across tanks and conditions. Uneaten food and faeces were removed from the tanks at least three times per week to prevent organic build-up.

Thermal treatment

Following acclimatisation, zebrafish were exposed to constant elevated or low temperatures. Tank water was gradually adjusted from 26 °C to either 34 °C (elevated temperature) or 18 °C (low temperature) over a 72-hour period, with controlled steps of ± 2 °C every 16 h. Fish were then maintained at their respective constant temperatures (34 ± 1 °C, 26 ± 1 °C or 18 ± 1 °C) for 21 consecutive days. Each tank was assigned to one temperature condition only, and thus represents a single experimental unit (i.e., one biological replicate per group) which is a limitation of our study warranting careful interpretation of our findings. These thermal regimes were selected based on prior studies, as they fall within the thermal tolerance limits of zebrafish and mimic ecologically relevant high and low environmental conditions[30], as discussed in the Introduction section.

The three tanks were placed side by side, and standardised for internal setup and environmental parameters, including lighting (14:10 h light/dark cycle), filtration, aeration, and heating. Fish were fed three times daily (10:00 AM, 2:00 PM, and 6:00 PM) with the same commercial diet, delivered via automatic feeders. To

accommodate potential differences in metabolic rate between temperature groups, fish were allowed to feed ad libitum, ensuring they could meet their own nutritional demands, which may vary under different thermal conditions. Behavioural observations were performed daily for five minutes by trained observers to monitor welfare indicators.

Sample collection

At the end of the 21-day exposure, fish were euthanised with tricaine methanesulphonate (MS-222, 300 mg/L), followed by decapitation to collect both eyes. For each tank (i.e., each temperature group), four pools of eyes were prepared, each consisting of both eyes from eight randomly selected fish ($n = 8$ fish per pool, 4 pools per tank).

Because fish were drawn from the same mixed-sex population with an approximately 1:1 sex ratio, and selection for pooling was fully random, each pool is expected to contain a balanced representation of males and females. Body mass was not recorded at the time of sampling because individuals displayed homogeneous body size at baseline, and differences in final body mass are expected under thermal challenges due to temperature-dependent modulation of metabolic rate, even when fish are allowed to feed ad libitum. Moreover, previous studies investigating zebrafish responses to altered thermal regimes[28] have similarly not included post-exposure body size measurements, reflecting a common methodological approach in this experimental context.

These pools represent biological variation at the individual level but originate from the same tank and therefore do not constitute independent biological replicates. Throughout the experimental period, no mortality or overt signs of poor health were observed in any of the groups. No macroscopic morphological anomalies were observed in the eyes under any experimental condition.

To minimise potential time-of-day effects on the eye proteome, samples were collected over a five-hour period (10 AM–15 PM) by alternating individuals from the different temperature groups. This sampling strategy ensured a homogeneous distribution of samples across the time window and reduced the likelihood of systematic bias linked to circadian or time-specific variations. Tissues were immediately immersed in PBS containing protease inhibitors (Roche, Basel, Switzerland), snap-frozen on dry ice, and stored at −80 °C for proteomic analysis.

To ensure blinding at different stages of the experiment, the procedures were carried out by independent researchers at separate institutions. Animal housing, thermal exposure, and tissue collection were performed by M.T. and F.F. at the University of Bologna. Samples were anonymised with codes that did not reveal treatment allocation and transferred to another institution. Proteomic analysis was conducted in a blinded manner by E.M., S.N., F.G.S., J.G., and G.T., who remained unaware of the experimental groups throughout the analysis.

Ethics declarations

All procedures were conducted in accordance with ethical guidelines and were approved by the institutional Animal Care Committee and the Italian Ministry of Health (protocol number 290/2017-PR). The study is reported in compliance with the ARRIVE guidelines. No experimental subject died during housing or during the thermal treatments.

Proteomic analysis

Proteomic analysis of zebrafish eyes was performed after 21 days of constant temperature exposure. Eye samples, consisting of pools from eight fish were analysed using a shotgun label-free proteomic approach for the identification and quantification of expressed proteins.

Each eye sample was homogenised using a Potter homogeniser in 100 µl of extraction buffer (8 M urea, 20 mM Hepes pH 8, with protease inhibitors Complete Mini), on ice, at full speed for 10 s. The homogenate was centrifuged at 15,000 rpm for 10 min at 4 °C to remove unhomogenised tissue and large cellular debris. The pellet was discarded, and the protein concentration of the supernatant was determined using the Bradford assay (Sigma-Aldrich, Milan, Italy) with bovine serum albumin as the standard[89].

Prior to proteolysis, proteins were reduced with 13 mM dithioerythritol (DTE; 15 min at 50 °C) and alkylated with 26 mM iodoacetamide (IAA; 30 min at room temperature, in the dark). Protein digestion was carried out using sequence-grade trypsin (Promega, Milan, Italy) for 16 h at 37 °C with a protein to enzyme ratio of 20:1.

The proteolytic digests were desalted using Zip-Tip C18 (Millipore, Milan, Italy) before mass spectrometric (MS) analysis[90].

NanoHPLC coupled to MS/MS analysis was performed on a Dionex Ultimate 3000 HPLC system with an EASY-SprayTM 2 µm 15 cm × 150 µm capillary column packed with 2 µm C18 100 Å particles, connected to a Q-Exactive Plus Orbitrap (Thermo Fisher Scientific, Waltham, MA, USA). MS spectra were acquired over an m/z range of 350–2000 Da at a resolution of 70,000, operating in data dependent mode. HCD MS/MS spectra were collected at a resolution of 17,500 for the 10 most abundant ions in each MS scan using a normalised collision energy of 35%, and an isolation window of 3 m/z. Rejection of + 1 and unassigned charge states were enabled[91]. Data acquisition was controlled by Xcalibur (Thermo Fisher Scientific, Monza (MI), Italy)[92]. The instrument was externally calibrated prior to each analytical sequence. A HeLa protein digest (Thermo Fisher Scientific) was injected as a quality control to monitor mass accuracy, chromatographic stability and signal intensity.

Parallel Reaction Monitoring (PRM) analysis was performed to validate selected proteins of functional relevance within key pathways identified by enrichment analysis, namely NADH dehydrogenase [ubiquinone] flavoprotein 1 (ndufv1), Cytochrome c oxidase subunit 6 C (cox6c), L-lactate dehydrogenase A chain (Idha), Long-wavelength-sensitive-1 cone opsin (opn1lw1), Opsin 1 (cone pigments), short-wave-sensitive 2 (opn1sw2), and S-arrestin (saga).

For PRM validation, at least two peptides were selected for each target protein, and nine transitions were monitored per peptide using Skyline software (https://skyline.ms/project/home/software/Skyline/begin.view,

version 25.1.0.142). MS^2 scans were triggered by an inclusion list from either ndufv1, cox6c, Idha, opn1lw1, opn1sw2, and saga peptides, without time scheduling. Data were acquired at a resolution of 35,000 with an AGC target value of 2×105, a maximum injection time of 100 ms, and an isolation window of 1.5 m/z. PRM raw data files were processed in Skyline against a protein sequence database of the six target proteins. Search parameters included trypsin digestion (maximum one missed cleavage sites), a minimum peptide length of six amino acids, and a mass tolerance of 20 ppm for precursor ions and 100 ppm for fragment ions. Carbamidomethylation of cysteine was set as a fixed modification, while deamidation of asparagine (Asn) and glutamine (Gln) was set as a variable modification. No internal standards were used, and the total peak area of each peptide was extracted for comparison across samples. Representative extracted-ion chromatograms (XICs) for each target protein are shown in Supplementary Fig. S3–S4, and representative MS^2 spectra are reported in Supplementary Fig. S5-S6.

Statistical and bioinformatic analysis of the proteomic data

MS spectra were searched against the *Danio rerio* UniProt sequence database (release 2023, 47,579 entries) using MaxQuant (version 1.6.1.0). The following parameters were used: initial maximum allowed mass deviation of 10 ppm for monoisotopic precursor ions and 0.5 Da for MS/MS peaks, trypsin enzyme specificity, a maximum of two missed cleavages, carbamidomethyl cysteine as fixed modification, N-terminal acetylation, methionine oxidation and asparagine/glutamine deamidation as variable modifications. False protein identification rate (5%) was estimated by searching MS/MS spectra against the corresponding reversed-sequence (decoy) database. Minimum required peptide length was set to 7 amino acids and minimum number of unique peptide supporting protein identification was set to 1. Quantification in MaxQuant was performed using the built-in LFQ algorithms based on extracted ion intensity of precursor ions. The coefficient of variation (CV%) of LFQ (Label-Free Quantification) intensities among technical replicates was below 12%, confirming good quantitative reproducibility across runs.

Four pools of eyes (from eight animals each) were analysed per temperature group (elevated: 34 °C; control; 26 °C; low: 18 °C). Only proteins detected in at least three out of four pools per group were included in statistical analyses, and no missing-value imputation was applied.

Statistical analyses of Max Quant results were performed using the Perseus software module (version 1.5.5.3). Principal component analysis-based multiconfidence ellipse analysis, PCA, was carried out on quantitative data related to proteins expressed at the three different thermal treatments using the SRplot web tool (https://www.bioinformatics.com.cn/srplot). Prior to multivariate analysis of variance (MANOVA), data distribution was evaluated using the Shapiro-Wilk test, which indicated deviations from perfect normality ($W = 0.63–0.68$), an expected feature of proteomic datasets with wide dynamic ranges. Multivariate analysis of variance (MANOVA) was conducted using Paleontological Statistics (PAST) software package[93]. Focusing on specific comparisons, namely 34 °C vs. 26 °C and 18 °C vs. 26 °C, proteins were considered differentially expressed if they were exclusively present in one condition or showed significant t-test difference (Student's test FDR ≤ 0.05). No additional fold-change threshold was applied.

Bioinformatic analyses were carried out by CLUEGO software (Cytoscape release 3.8.2)[94], and an Ingenuity Pathway Analysis (IPA, release 2024, QIAGEN Inc., https://www.qiagenbioinformatics.com/products/ingenuity pathway-analysis) to cluster enriched annotation groups of biological processes, pathways, and networks within the set of identified proteins using *Danio rerio* as data base. Functional grouping was based on Fischer's exact test (p-value ≤ 0.05 and at least 3 counts per category) in GLUEGO and P-value (Benjamini-Hochberg adjusted p-value) ≤ 0.05 (-log (p-value) cutoff of 1.3) in IPA.

Data availability

The mass spectrometry proteomics data have been deposited to the ProteomeXchange Consortium via the PRIDE partner repository, with the dataset identifier PXD061443.

Received: 23 July 2025; Accepted: 19 November 2025
Published online: 29 November 2025

References

1. Richardson, R., Tracey-White, D., Webster, A. & Moosajee, M. The zebrafish eye-a paradigm for investigating human ocular genetics. *Eye* **31**, 68–86. https://doi.org/10.1038/eye.2016.198 (2017).
2. Stenkamp, D. L. Development of the vertebrate eye and retina. *Prog. Mol. Biol. Transl. Sci.* **134**, 397–414. https://doi.org/10.1016/bs.pmbts.2015.06.006 (2015).
3. Graw, J. Eye development. *Curr. Top. Dev. Biol.* **90**, 343–386. https://doi.org/10.1016/S0070-2153(10)90010-0 (2010).
4. Trost, A., Bruckner, D., Rivera, F. J. & Reitsamer, H. A. Pericytes in the retina. *Adv. Exp. Med. Biol.* **1122**, 1–26. https://doi.org/10.1007/978-3-030-11093-2_1 (2019).
5. Trost, A. et al. Brain and Retinal Pericytes: Origin, Function and Role. *Front. Cell. Neurosci.* https://doi.org/10.3389/fncel.2016.00020 (2016).
6. Semba, R. D., Enghild, J. J., Venkatraman, V., Dyrlund, T. F. & Van Eyk, J. E. The human eye proteome project: perspectives on an emerging proteome. *Proteomics* **13**, 2500–2511. https://doi.org/10.1002/pmic.201300075 (2013).
7. Ahmad, M. T., Zhang, P., Dufresne, C., Ferrucci, L. & Semba, R. D. The human eye proteome project: updates on an emerging proteome. *Proteomics* **18**, e1700394. https://doi.org/10.1002/pmic.201700394 (2018).
8. Semba, R. D. & Enghild, J. J. Proteomics and the eye. *Proteomics. Clin. Appl.* **8**, 127–129. https://doi.org/10.1002/prca.201470024 (2014).
9. Koronyo, Y. et al. Retinal pathological features and proteome signatures of Alzheimer's disease. *Acta Neuropathol.* **145**, 409–438. https://doi.org/10.1007/s00401-023-02548-2 (2023).
10. Heilenbach, N. et al. Environmental influences on ophthalmic conditions: A scoping review. *Clin. Exp. Ophthalmol.* **51**, 516–545. https://doi.org/10.1111/ceo.14262 (2023).
11. Hsu, S. T., Ponugoti, A., Deaner, J. D. & Vajzovic, L. Update on retinal drug toxicities. *Curr. Ophthalmol. Rep.* **9**, 168–177. https://doi.org/10.1007/s40135-021-00277-x (2021).

12. Choi, T. Y., Choi, T. I., Lee, Y. R., Choe, S. K. & Kim, C. H. Zebrafish as an animal model for biomedical research. *Exp. Mol. Med.* **53**, 310–317. https://doi.org/10.1038/s12276-021-00571-5 (2021).
13. Villamizar, N., Vera, L. M., Foulkes, N. S. & Sanchez-Vazquez, F. J. Effect of lighting conditions on zebrafish growth and development. *Zebrafish* **11**, 173–181. https://doi.org/10.1089/zeb.2013.0926 (2014).
14. Cassar, S., Dunn, C. & Ramos, M. F. Zebrafish as an animal model for ocular toxicity testing: A review of ocular anatomy and functional assays. *Toxicol. Pathol.* **49**, 438–454. https://doi.org/10.1177/0192623320964748 (2021).
15. Yi, J. et al. Rapid Assessment of Ocular Toxicity from Environmental Contaminants Based on Visually Mediated Zebrafish Behavior Studies. *Toxics* https://doi.org/10.3390/toxics11080706 (2023).
16. Saputra, F., Pramata, A. D., Soegianto, A. & Hu, S. Y. Vitamin E mitigates polystyrene-nanoplastic-induced visual dysfunction in zebrafish larvae. *Int. J. Mol. Sci.* https://doi.org/10.3390/ijms26031216 (2025).
17. Saputra, F., Kishida, M. & Hu, S. Y. Nitrate and Nitrite Exposure Induces Visual Impairments in Adult Zebrafish. *Toxics* https://doi.org/10.3390/toxics12070518 (2024).
18. Aslanidi, K. B. & Kharakoz, D. P. Limits of temperature adaptation and thermopreferendum. *Cell. bioscience* https://doi.org/10.1186/s13578-021-00574-9 (2021).
19. Schaefer, J. & Ryan, A. Developmental plasticity in the thermal tolerance of zebrafish *Danio rerio*. *J. Fish Biol.* **69**, 722–734. https://doi.org/10.1111/j.1095-8649.2006.01145.x (2006).
20. Cortemeglia, C. & Beitinger, T. L. Temperature tolerances of Wild-Type and red Transgenic zebra Danios. *Trans. Am. Fish. Soc.* **134**, 1431–1437. https://doi.org/10.1577/T04-197.1 (2005).
21. Parichy, D. M. Advancing biology through a deeper understanding of zebrafish ecology and evolution. *eLife* https://doi.org/10.7554/eLife.05635 (2015).
22. Spence, R., Gerlach, G., Lawrence, C. & Smith, C. The behaviour and ecology of the zebrafish, *Danio rerio*. *Biol. Rev. Camb. Philos. Soc.* **83**, 13–34. https://doi.org/10.1111/j.1469-185X.2007.00030.x (2008).
23. Engeszer, R. E., Patterson, L. B., Rao, A. A. & Parichy, D. M. Zebrafish in the wild: a review of natural history and new notes from the field. *Zebrafish* **4**, 21–40. https://doi.org/10.1089/zeb.2006.9997 (2007).
24. Arunachalam, M., Raja, M., Vijayakumar, C., Malaiammal, P. & Mayden, R. L. Natural history of zebrafish (*Danio rerio*) in India. *Zebrafish* **10**, 1–14. https://doi.org/10.1089/zeb.2012.0803 (2013).
25. López-Olmeda, J. F. & Sánchez-Vázquez, F. J. Thermal biology of zebrafish (*Danio rerio*). *J. Therm. Biol.* **36**, 91–104. https://doi.org/10.1016/j.jtherbio.2010.12.005 (2011).
26. Nonnis, S. et al. Acute environmental temperature variation affects brain protein expression, anxiety and explorative behaviour in adult zebrafish. *Sci. Rep.* **11**, 2521. https://doi.org/10.1038/s41598-021-81804-5 (2021).
27. Angiulli, E. et al. Increase in environmental temperature affects exploratory behaviour, anxiety and social preference in *Danio rerio*. *Sci. Rep.* **10**, 5385. https://doi.org/10.1038/s41598-020-62331-1 (2020).
28. Toni, M. et al. Environmental temperature variation affects brain protein expression and cognitive abilities in adult zebrafish (*Danio rerio*): A proteomic and behavioural study. *J. Proteom.* https://doi.org/10.1016/j.jprot.2019.103396 (2019).
29. Toni, M., Frabetti, F., Tedeschi, G. & Alleva, E. Effects of Environmental Temperature Variation on the Spatio-Temporal Shoaling Behaviour of Adult Zebrafish (*Danio rerio*): A Two- and Three-Dimensional Analysis. *Animals: open. access. J. MDPI* https://doi.org/10.3390/ani15142006 (2025).
30. Vergauwen, L., Benoot, D., Blust, R. & Knapen, D. Long-term warm or cold acclimation elicits a specific transcriptional response and affects energy metabolism in zebrafish. *Comp. Biochem. Physiol. A Mol. Integr. Physiol.* **157**, 149–157. https://doi.org/10.1016/j.cbpa.2010.06.160 (2010).
31. Maffioli, E. et al. Brain Proteome and Behavioural Analysis in Wild Type, BDNF$^{(+/-)}$ and BDNF$^{(-/-)}$ Adult Zebrafish (*Danio rerio*) Exposed to Two Different Temperatures. *Int. J. Mol. Sci.* https://doi.org/10.3390/ijms23105606 (2022).
32. Maffioli, E. et al. Environmental temperature variation affects brain lipid composition in adult zebrafish (*Danio rerio*). *Int. J. Mol. Sci.* **25**, 9629 (2024).
33. Maffioli, E. et al. The Neurotoxic Effect of Environmental Temperature Variation in Adult Zebrafish (*Danio rerio*). *Int. J. Mol. Sci.* https://doi.org/10.3390/ijms242115735 (2023).
34. Toni, M., Arena, C., Cioni, C. & Tedeschi, G. Temperature- and chemical-induced neurotoxicity in zebrafish. *Front. Physiol.* **14**, 1276941. https://doi.org/10.3389/fphys.2023.1276941 (2023).
35. Gal-Ben-Ari, S., Barrera, I., Ehrlich, M. & Rosenblum, K. PKR: A kinase to remember. *Front. Mol. Neurosci.* **11**, 480. https://doi.org/10.3389/fnmol.2018.00480 (2018).
36. Dabo, S. & Meurs, E. F. dsRNA-dependent protein kinase PKR and its role in stress, signaling and HCV infection. *Viruses* **4**, 2598–2635. https://doi.org/10.3390/v4112598 (2012).
37. Zhao, M. et al. Double-stranded RNA-dependent protein kinase (pkr) is essential for thermotolerance, accumulation of HSP70, and stabilization of ARE-containing HSP70 mRNA during stress. *J. Biol. Chem.* **277**, 44539–44547. https://doi.org/10.1074/jbc.M208408200 (2002).
38. Sauve, A. A., Wolberger, C., Schramm, V. L. & Boeke, J. D. The biochemistry of sirtuins. *Annu. Rev. Biochem.* **75**, 435–465. https://doi.org/10.1146/annurev.biochem.74.082803.133500 (2006).
39. Zhou, M., Luo, J. & Zhang, H. Role of Sirtuin 1 in the pathogenesis of ocular disease (Review). *Int. J. Mol. Med.* **42**, 13–20. https://doi.org/10.3892/ijmm.2018.3623 (2018).
40. Sheng, W. et al. Effect of Resveratrol on Sirtuins, OPA1, and Fis1 expression in adult zebrafish retina. *Investig. Ophthalmol. Vis. Sci.* **59**, 4542–4551. https://doi.org/10.1167/iovs.18-24539 (2018).
41. Qin, W. et al. Neuronal SIRT1 activation as a novel mechanism underlying the prevention of Alzheimer disease amyloid neuropathology by calorie restriction. *J. Biol. Chem.* **281**, 21745–21754. https://doi.org/10.1074/jbc.M602909200 (2006).
42. Dai, J. M., Wang, Z. Y., Sun, D. C., Lin, R. X. & Wang, S. Q. SIRT1 interacts with p73 and suppresses p73-dependent transcriptional activity. *J. Cell. Physiol.* **210**, 161–166. https://doi.org/10.1002/jcp.20831 (2007).
43. Luo, J. et al. Negative control of p53 by Sir2alpha promotes cell survival under stress. *Cell* **107**, 137–148. https://doi.org/10.1016/s0092-8674(01)00524-4 (2001).
44. Vaziri, H. et al. hSIR2(SIRT1) functions as an NAD-dependent p53 deacetylase. *Cell* **107**, 149–159. https://doi.org/10.1016/s0092-8674(01)00527-x (2001).
45. Cohen, H. Y. et al. Calorie restriction promotes mammalian cell survival by inducing the SIRT1 deacetylase. *Science* **305**, 390–392. https://doi.org/10.1126/science.1099196 (2004).
46. Zhao, K., Zhang, H. & Yang, D. SIRT1 exerts protective effects by inhibiting Endoplasmic reticulum stress and NF-kappaB signaling pathways. *Front. cell. Dev. Biology*. **12**, 1405546. https://doi.org/10.3389/fcell.2024.1405546 (2024).
47. Prola, A. et al. SIRT1 protects the heart from ER stress-induced cell death through eIF2alpha deacetylation. *Cell Death Differ.* **24**, 343–356. https://doi.org/10.1038/cdd.2016.138 (2017).
48. Ghosh, H. S., Reizis, B. & Robbins, P. D. SIRT1 associates with eIF2-alpha and regulates the cellular stress response. *Sci. Rep.* **1**, 150. https://doi.org/10.1038/srep00150 (2011).
49. Harding, H. P. et al. An integrated stress response regulates amino acid metabolism and resistance to oxidative stress. *Mol. Cell.* **11**, 619–633. https://doi.org/10.1016/s1097-2765(03)00105-9 (2003).
50. Donnelly, N., Gorman, A. M., Gupta, S. & Samali, A. The eIF2alpha kinases: their structures and functions. *Cell. Mol. Life Sci.* **70**, 3493–3511. https://doi.org/10.1007/s00018-012-1252-6 (2013).

51. Chen, H. Y. et al. Musashi-1 promotes chemoresistant granule formation by PKR/eIF2alpha signalling cascade in refractory glioblastoma. *Biochim. Et Biophys. Acta Mol. Basis Disease*. **1864**, 1850–1861. https://doi.org/10.1016/j.bbadis.2018.02.017 (2018).
52. Lopez-Grancha, M. et al. A novel selective PKR inhibitor restores cognitive deficits and neurodegeneration in Alzheimer disease experimental models. *J. Pharmacol. Exp. Ther.* **378**, 262–275. https://doi.org/10.1124/jpet.121.000590 (2021).
53. Elvira, R., Cha, S. J., Noh, G. M., Kim, K. & Han, J. PERK-Mediated eIF2alpha Phosphorylation Contributes to The Protection of Dopaminergic Neurons from Chronic Heat Stress in Drosophila. *Int. J. Mol. Sci.* https://doi.org/10.3390/ijms21030845 (2020).
54. Williams, T. D. & Rousseau, A. Translation regulation in response to stress. *FEBS J.* **291**, 5102–5122. https://doi.org/10.1111/febs.17076 (2024).
55. Wek, R. C. Role of eIF2alpha Kinases in Translational Control and Adaptation to Cellular Stress. *Cold Spring Harbor perspect. biol.* https://doi.org/10.1101/cshperspect.a032870 (2018).
56. Hsiao, Y. T. et al. Presynaptic SNAP-25 regulates retinal waves and retinogeniculate projection via phosphorylation. *Proc. Natl. Acad. Sci. U.S.A.* **116**, 3262–3267. https://doi.org/10.1073/pnas.1812169116 (2019).
57. Abokyi, S. & Tse, D. Y. Age-related driving mechanisms of retinal diseases and neuroprotection by transcription factor EB-targeted therapy. *Neural Regeneration Res.* **20**, 366–377. https://doi.org/10.4103/NRR.NRR-D-23-02033 (2025).
58. Tang, B. L. Sirt1 and the mitochondria. *Mol. Cells*. **39**, 87–95. https://doi.org/10.14348/molcells.2016.2318 (2016).
59. Bause, A. S. & Haigis, M. C. SIRT3 regulation of mitochondrial oxidative stress. *Exp. Gerontol.* **48**, 634–639. https://doi.org/10.1016/j.exger.2012.08.007 (2013).
60. Zhang, Q., Siyuan, Z., Xing, C. & Ruxiu, L. SIRT3 regulates mitochondrial function: A promising star target for cardiovascular disease therapy. *Biomed. pharmacotherapy = Biomedecine Pharmacotherapie*. **170**, 116004. https://doi.org/10.1016/j.biopha.2023.116004 (2024).
61. Zhang, J. et al. Mitochondrial Sirtuin 3: new emerging biological function and therapeutic target. *Theranostics* **10**, 8315–8342. https://doi.org/10.7150/thno.45922 (2020).
62. Liu, Z. et al. Chronic heat stress inhibits glycogen synthesis through gga-miR-212-5p/GYS1 axis in the breast muscle of broilers. *Poult. Sci.* **103**, 103455. https://doi.org/10.1016/j.psj.2024.103455 (2024).
63. Zhang, Z. Y. et al. Effects of constant and Cyclic heat stress on muscle metabolism and meat quality of broiler breast fillet and thigh meat. *Poult. Sci.* **91**, 2931–2937. https://doi.org/10.3382/ps.2012-02255 (2012).
64. Sajjanar, B. et al. Cross-talk between energy metabolism and epigenetics during temperature stress response in C2C12 myoblasts. *Int. J. Hyperthermia: Official J. Eur. Soc. Hyperthermic Oncol. North. Am. Hyperth. Group.* **36**, 776–784. https://doi.org/10.1080/02656736.2019.1639834 (2019).
65. Okawa, H., Sampath, A. P., Laughlin, S. B. & Fain, G. L. ATP consumption by mammalian rod photoreceptors in darkness and in light. *Curr. Biology: CB*. **18**, 1917–1921. https://doi.org/10.1016/j.cub.2008.10.029 (2008).
66. Country, M. W. Retinal metabolism: A comparative look at energetics in the retina. *Brain Res.* **1672**, 50–57. https://doi.org/10.1016/j.brainres.2017.07.025 (2017).
67. Wong-Riley, M. T. Energy metabolism of the visual system. *Eye Brain*. **2**, 99–116. https://doi.org/10.2147/EB.S9078 (2010).
68. Kam, J. H. & Jeffery, G. To unite or divide: mitochondrial dynamics in the murine outer retina that preceded age related photoreceptor loss. *Oncotarget* **6**, 26690–26701. https://doi.org/10.18632/oncotarget.5614 (2015).
69. Ingram, N. T., Fain, G. L. & Sampath, A. P. Elevated energy requirement of cone photoreceptors. *Proc. Natl. Acad. Sci. U.S.A.* **117**, 19599–19603. https://doi.org/10.1073/pnas.2001776117 (2020).
70. Heidelberger, R., Thoreson, W. B. & Witkovsky, P. Synaptic transmission at retinal ribbon synapses. *Prog. Retin. Eye Res.* **24**, 682–720. https://doi.org/10.1016/j.preteyeres.2005.04.002 (2005).
71. Hurley, J. B., Lindsay, K. J. & Du, J. Glucose, lactate, and shuttling of metabolites in vertebrate retinas. *J. Neurosci. Res.* **93**, 1079–1092. https://doi.org/10.1002/jnr.23583 (2015).
72. Deng, W. et al. Quantitative imaging of the clearance systems in the eye and the brain. *Quant. Imaging Med. Surg.* **10**, 1–14. https://doi.org/10.21037/qims.2019.11.18 (2020).
73. Boland, B. et al. Promoting the clearance of neurotoxic proteins in neurodegenerative disorders of ageing. *Nat. Rev. Drug Discov.* **17**, 660–688. https://doi.org/10.1038/nrd.2018.109 (2018).
74. Yang, J. & Zhang, C. Targeting the autophagy-lysosomal pathway in huntington disease: a Pharmacological perspective. *Front. Aging Neurosci.* **15**, 1175598. https://doi.org/10.3389/fnagi.2023.1175598 (2023).
75. Malampati, S. et al. Targeting Aggrephagy for the Treatment of Alzheimer's Disease. *Cells* https://doi.org/10.3390/cells9020311 (2020).
76. Bucca, G. et al. Translational control plays an important role in the adaptive heat-shock response of streptomyces coelicolor. *Nucleic Acids Res.* **46**, 5692–5703. https://doi.org/10.1093/nar/gky335 (2018).
77. Williams, T. D. & Rousseau, A. Translation regulation in response to stress. *FEBS J.* **291**, 5102–5122. https://doi.org/10.1111/febs.17076 (2024).
78. Bosch-Presegue, L. & Vaquero, A. Sirtuins in stress response: guardians of the genome. *Oncogene* **33**, 3764–3775. https://doi.org/10.1038/onc.2013.344 (2014).
79. Lin, S. et al. Sirtuins in mitochondrial stress: indispensable helpers behind the scenes. *Ageing Res. Rev.* **44**, 22–32. https://doi.org/10.1016/j.arr.2018.03.006 (2018).
80. Vasquez, M. C., Beam, M., Blackwell, S., Zuzow, M. J. & Tomanek, L. Sirtuins regulate proteomic responses near thermal tolerance limits in the blue mussels *Mytilus galloprovincialis* and *Mytilus trossulus*. *J. Exp. Biol.* **220**, 4515–4534. https://doi.org/10.1242/jeb.160325 (2017).
81. Guderley, H. Metabolic responses to low temperature in fish muscle. *Biol. Rev. Camb. Philos. Soc.* **79**, 409–427. https://doi.org/10.1017/s1464793103006328 (2004).
82. O'Brien, K. M. Mitochondrial biogenesis in cold-bodied fishes. *J. Exp. Biol.* **214**, 275–285. https://doi.org/10.1242/jeb.046854 (2011).
83. Masland, R. H. The neuronal organization of the retina. *Neuron* **76**, 266–280. https://doi.org/10.1016/j.neuron.2012.10.002 (2012).
84. Herskovits, A. Z. & Guarente, L. Sirtuin deacetylases in neurodegenerative diseases of aging. *Cell Res.* **23**, 746–758. https://doi.org/10.1038/cr.2013.70 (2013).
85. Chung, D. J. & Schulte, P. M. Mitochondria and the thermal limits of ectotherms. *J. Exp. Biol.* https://doi.org/10.1242/jeb.227801 (2020).
86. Goldman, D. Muller glial cell reprogramming and retina regeneration. *Nat. Rev. Neurosci.* **15**, 431–442. https://doi.org/10.1038/nrn3723 (2014).
87. Wan, J. & Goldman, D. Retina regeneration in zebrafish. *Curr. Opin. Genet. Dev.* **40**, 41–47. https://doi.org/10.1016/j.gde.2016.05.009 (2016).
88. De Schutter, J. D. et al. Differential retinal ganglion cell resilience to optic nerve injury across vertebrate species. *Front. NeuroSci.* **19**, 1596464. https://doi.org/10.3389/fnins.2025.1596464 (2025).
89. Mortarino, M. et al. Two-dimensional polyacrylamide gel electrophoresis map of bull seminal plasma proteins. *Electrophoresis* **19**, 797–801. https://doi.org/10.1002/elps.1150190532 (1998).
90. Zambonelli, C. et al. Cloning and expression in *Escherichia coli* of the gene encoding streptomyces PMF PLD, a phospholipase D with high transphosphatidylation activity. *Enzym. Microb. Technol.* **33**, 676–688 (2003).
91. Capraro, J. et al. Internalisation and multiple phosphorylation of gamma-Conglutin, the lupin seed glycaemia-lowering protein, in HepG2 cells. *Biochem. Biophys. Res. Commun.* **437**, 648–652. https://doi.org/10.1016/j.bbrc.2013.07.026 (2013).

92. Tamplenizza, M. et al. Nitric oxide synthase mediates PC12 differentiation induced by the surface topography of nanostructured TiO2. *J. Nanobiotechnol.* https://doi.org/10.1186/1477-3155-11-35 (2013).
93. Hammer, Ø., Harper, D. A. T. & Ryan, P. D. Past: paleontological statistics software package for education and data analysis. *Palaeontol. Electron.* **4**, XIX–XX (2001).
94. Shannon, P. et al. Cytoscape: a software environment for integrated models of biomolecular interaction networks. *Genome Res.* **13**, 2498–2504. https://doi.org/10.1101/gr.1239303 (2003).

Author contributions

Conceptualization, G.T. and M.T.; methodology, A.N., E.M., G.T., J.G., M.T. and S.N.; housing and maintaining animals: F.F.; software, A.N., E.M., F.G.S., M.T., S.N. and G.T.; formal analysis, E.M., G.T., M.T. and S.N.; investigation, G.T. and M.T.; resources, G.T. and M.T.; data curation, F.G.S., G.T., M.T. and S.N; writing—original draft preparation, G.T. and M.T.; writing—review and editing, E.M., F.F., G.T., M.T. and S.N.; visualization, G.T. and M.T.; supervision, G.T. and M.T.; project administration, G.T. and M.T.; funding acquisition, G.T. and M.T. All authors reviewed the manuscript.

Funding

This research was funded by Sapienza University of Rome (Progetti di Ricerca RM12117A383FC177, RD12318A998C70B8, and RM1221815DB5BC08).

Declarations

Competing interests

The authors declare no competing interests.

Additional information

Supplementary Information The online version contains supplementary material available at https://doi.org/10.1038/s41598-025-29745-1.

Correspondence and requests for materials should be addressed to G.T. or M.T.

Reprints and permissions information is available at www.nature.com/reprints.

Publisher's note Springer Nature remains neutral with regard to jurisdictional claims in published maps and institutional affiliations.